

Nonmonotonic $d_{x^2-y^2}$ -Wave Superconductivity in Electron-Doped Cuprates Viewing from the Strong-Coupling Side

Tsutomu WATANABE^{1,2*}, Takafumi MIYATA¹, Hisatoshi YOKOYAMA³, Yukio TANAKA^{1,2} and Jun-ichiro INOUE¹

¹*Department of Applied Physics, Nagoya University, Nagoya 464-8603*

²*CREST Japan Science and Technology Corporation (JST)*

³*Department of Physics, Tohoku University, Sendai 980-8578*

Applying a variational Monte Carlo method to a two-dimensional t - J model, we study the nonmonotonic $d_{x^2-y^2}$ -wave superconductivity, observed by Raman scattering and ARPES experiments in the electron-doped cuprates. As a gap function in the trial state, we extend the d -wave form (ext. d) so as to have its maxima located near the hot spots of the system. It is found that, in contrast to the hole-doped case, the ext. d wave is always more stable than the simple d wave in the electron-doped case, and the magnetic correlation of the wave vector (π, π) as well as the pair correlation is enhanced. These results corroborate spin-correlation-mediated superconductivity in cuprates, recently argued from a FLEX calculation. In addition, we confirm that s - and p -wave symmetries are never stabilized even in the over-doped regime.

KEYWORDS: superconductivity, electron-doped High- T_c cuprate, nonmonotonic $d_{x^2-y^2}$ wave, antiferromagnetic correlation, hot spot, t - J model, variational Monte Carlo method

Introduction: Antiferromagnetic (AF) correlation is probably the primary origin to form Cooper pairs in the high- T_c cuprates.^{1,2} A recent neutron scattering experiment³ in the electron-doped (n -type) cuprates discovered peaks at magnetic Bragg spots in both normal and superconducting (SC) phases, which fact indicates that the spin correlation of the AF wave vector $\mathbf{Q} = (\pi, \pi)$ plays an important role in n -type cuprates.

As in the hole-doped (p -type) cuprates, the pairing symmetry of the n -type ones was ascertained to be a $d_{x^2-y^2}$ -wave type, as far as the doping rate δ is smaller than 0.15, by a scanning SQUID microscope⁴ and angle-resolved photoelectron spectroscopy (ARPES).^{5,6} However, recent experiments by Raman scattering⁷ and ARPES⁸ have concluded that the pairing symmetry in the n -type cuprates is not the typical $d_{x^2-y^2}$ wave characterized by $\Delta_{\mathbf{k}} \propto \cos k_x - \cos k_y$, but exhibits a non-monotonic behavior. Namely, the maximum of $\Delta_{\mathbf{k}}$ is located midway between the Brillouin-zone boundary $(\pi, 0)$ and the zone diagonal $(\pi/2, \pi/2)$. Furthermore, for $T > T_c$, pseudogap-like behavior⁹ or an AF gap¹⁰ arises at this midway locus, in contrast to the p -type cuprates, in which the gap maximum and pseudogap behavior take place around $(\pi, 0)$.

These results can be explained by the fact that the loci of the gap maximum in the p and n types roughly coincide with their respective hot spots—the intersection of the Fermi surface and the magnetic Brillouin zone boundary [See Fig. 1(a)]. This observation affords confirmatory evidence that the superconductivity in cuprates is induced by the spin correlation (or fluctuation) of the wave vector \mathbf{Q} , which connects the hot spots.

Theoretically, Yoshimura and Hirashima¹¹ recently treated this issue, applying a fluctuation exchange approximation (FLEX) to the Hubbard model. They obtained a non-monotonic behavior of $\Delta_{\mathbf{k}}$ and consistent

results of Raman spectral functions and spin susceptibility etc. with the experiments. Since the electron correlation is not weak even in the n -type cuprates, the results of FLEX, which is basically a weak-coupling theory, should be checked by complementary studies from the strong-coupling and low-carrier-density sides. In this paper, we study this issue, applying a variational Monte Carlo (VMC) method¹² to a t - J -type model. So far, taking this approach, various aspects of the cuprates have been elucidated on a strong-coupling footing.¹³

A secondary interest of this paper is possible variation of the pairing symmetry from d to s wave in the over-doped regime of n -type cuprates, observed by tunneling spectroscopy¹⁴ and measurement of magnetic penetration depth.¹⁵ Although a BCS-level calculation¹⁶ supports these experiments, one has to confirm this issue using a less biased approach.

Formulation: We consider a two-dimensional t - J model, $\mathcal{H} = \mathcal{H}_t + \mathcal{H}_J$ with $\mathcal{H}_t = -\sum_{(i,j)\sigma} t_{ij} \mathcal{P}_G (c_{i\sigma}^\dagger c_{j\sigma} + \text{H.c.}) \mathcal{P}_G$ and $\mathcal{H}_J = J \sum_{(i,j)} (\mathbf{S}_i \cdot \mathbf{S}_j - n_i n_j / 4)$, where $\mathcal{P}_G = \prod_j (1 - n_{j\uparrow} n_{j\downarrow})$, the value of J/t is fixed at 0.3, and $t_{ij} = t, t', t''$ or 0, according as the site i is a first-, second-, third-nearest neighbor or farther site of the site j , respectively. An electron-doped (more-than-half-filled) system can be treated with a t - J model as a less-than-half-filled case, by applying a particle-hole transformation $c_{j\sigma}^\dagger \rightarrow \exp(i\mathbf{Q} \cdot \mathbf{r}_j) h_{j\sigma}$ with $t'(t'') \rightarrow -t'(-t'')$. Thus, we put $t'/t > 0$ (< 0) and $t''/t < 0$ (> 0) for n - (p -)type cuprates. Actually, we adopt typical values¹⁷ of t'/t and t''/t given in the caption of Fig. 1.

To this model, we apply a VMC method, which accurately treats the local correlation \mathcal{P}_G . As a variational function for a SC state, a simple Gutzwiller-type wave function is used,

$$|\Psi_{\text{SC}}\rangle = \mathcal{P}_G |\Phi_{\text{BCS}}\rangle = \mathcal{P}_G \left(\sum_{\mathbf{k}} \varphi_{\mathbf{k}} c_{\mathbf{k}\uparrow}^\dagger c_{-\mathbf{k}\downarrow}^\dagger \right)^{\frac{N_0}{2}} |0\rangle, \quad (1)$$

*E-mail: h042203d@mbox.nagoya-u.ac.jp

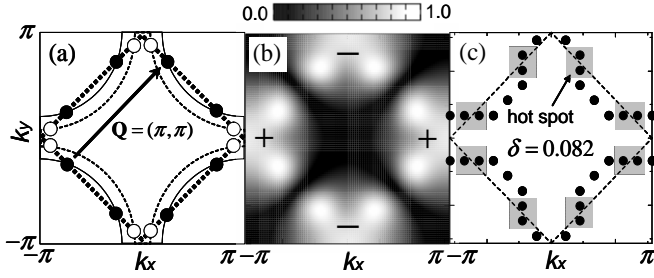


Fig. 1. (a) Hot spots are compared between a hole-doped ($t'/t = -0.1$, $t''/t = 0.1$, open circle) and an electron-doped ($t'/t = -0.16$, $t''/t = 0.2$, solid circle) cases for the optimal doping ($\delta = 0.15$). The bare Fermi surface for the former (latter) parameter set is denoted by a thin-dashed (solid) line, and the magnetic Brillouin zone boundary by a bold dotted line. The AF nesting vector \mathbf{Q} links two hot spots. (b) Pairing potential $\Delta_{\mathbf{k}}/t$ of the ext. d wave for the optimized parameter values (see text) of the system shown in (c). (c) The k -points on the Fermi surface for an underdoped density on a 14×14 lattice are shown with solid circles. Regions near the hot spots are indicated by shadows, and the magnetic Brillouin zone boundary by a dashed line.

with

$$\varphi_{\mathbf{k}} = \frac{u_{\mathbf{k}}}{v_{\mathbf{k}}} = \frac{\Delta_{\mathbf{k}}}{\varepsilon_{\mathbf{k}} - \mu + \sqrt{(\varepsilon_{\mathbf{k}} - \mu)^2 + \Delta_{\mathbf{k}}^2}}. \quad (2)$$

Here, Φ_{BCS} is the BCS wave function of a fixed particle number N_e , $\varepsilon_{\mathbf{k}} = -2t(\cos k_x + \cos k_y) - 4t' \cos k_x \cos k_y - 2t''(\cos 2k_x + \cos 2k_y)$, and the parameter μ is substituted by the chemical potential of the non-interacting case. It is already known that this type of wave function works well for t - J -type models.^{18,19} Anisotropy of the pairing potential is introduced into $\Delta_{\mathbf{k}}$, as $\Delta_{\mathbf{k}}^d = \Delta_0(\cos k_x - \cos k_y)$ for the simple d wave. We extend it so that it may have large amplitude near the hot spots,

$$\begin{aligned} \Delta_{\mathbf{k}}^{\text{ext}.d} &= \Delta_{\mathbf{k}}^d \\ &+ a\Delta_0 \left[k_y^2 e^{-c(k_x-b)^2 - dk_y^2} + k_y^2 e^{-c(k_x+b)^2 - dk_y^2} \right. \\ &- \left. k_x^2 e^{-c(k_y-b)^2 - dk_x^2} - k_x^2 e^{-c(k_y+b)^2 - dk_x^2} \right], \quad (3) \end{aligned}$$

and call it the extended- d (ext. d) wave. In $\Delta_{\mathbf{k}}^{\text{ext}.d}$, we add to $\Delta_{\mathbf{k}}^d$ eight Gaussian peaks, whose height, position and width in two directions are adjusted by parameter a, b, c and d , respectively. Although $\Delta_{\mathbf{k}}$ should be determined variationally, for simplicity we fix the parameters for the Gaussian, except for trial calculations,²⁰ at rough optimal values of the case $\delta = 0.082$ ($L = 14$), namely, $a = 3$, $b = 2$, $c = 1$ and $d = 1$; $\Delta_{\mathbf{k}}$ thereof is shown in Fig.1(b). Note that the loci of the maximal $\Delta_{\mathbf{k}}$ are situated very closely to the hot spots, shown in Fig.1(c). Thus, Δ_0 (amplitude of $\Delta_{\mathbf{k}}$) becomes a sole parameter to be optimized. Unlike the BCS theory, $\Delta_{\mathbf{k}}$ here is not entirely equivalent to the SC gap, especially in Δ_0 , but the symmetry of $\Delta_{\mathbf{k}}$ faithfully reflects the SC gap.

We have followed a conventional VMC scheme,¹² and collected 10^5 - 10^6 samples, which suppress the statistical errors in energy at $\sim 10^{-4}t$. The system used has $L \times L$ sites ($L = 12, 14$ and 16) with the periodic-antiperiodic boundary conditions. The particle density δ is chosen so as to satisfy the closed-shell condition.

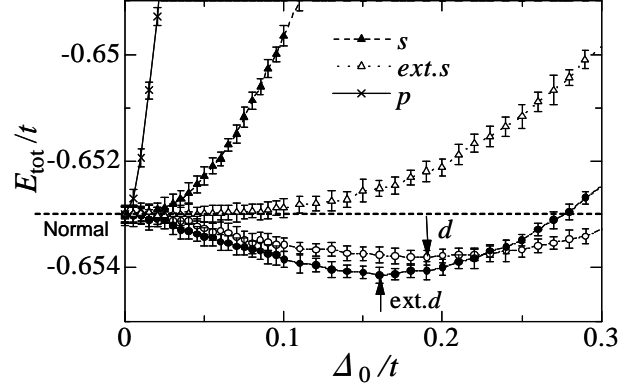


Fig. 2. Total energies versus a variational parameter Δ_0 for various pairing symmetries for an electron-doped system with $\delta = 0.163$. The arrows on the d and ext. d waves denote the optimal values. The value of the normal state ($\Delta_0 = 0$) is shown with a dashed line. The system is of 14×14 , and $J/|t| = 0.3$.

Results: Before going to the d -type pairings, we check the stability of the singlet s - ($\Delta_{\mathbf{k}} = \Delta_0$), ext. s - [$= \Delta_0(\cos k_x + \cos k_y)$] and triplet p -wave ($= \Delta_0 \sin k_x$) symmetries. In Fig. 2, the variational energies E_{tot} of the symmetries we treat are compared in the overdoped regime. Here, E_{tot} 's of the s , ext. s and p waves monotonically increase, as Δ_0 increases, and are destabilized with respect to the normal state. We have also confirmed that the same behavior persists to a large doping rate, $\delta = 0.245$, where SC states are no longer stabilized. Since our treatment is little biased in comparing pairing symmetries, we are confident that the p and s -type waves are not realized even in the overdoped regime; thus a pairing-symmetry transition is unlikely to arise.²¹

Now, we turn to the d -type symmetries. By contrast, the variational energies of the d - and ext. d -wave SC states plotted in Fig. 2 have minima at finite values of Δ_0 , as indicated by arrows. The decrease in E_{tot} of the $d_{x^2-y^2}$ wave has been well-known for the plain t - J model ($t' = t'' = 0$) since the early stage.²⁵ It should be noted here that the ext. d wave has an appreciably lower energy than the simple d wave even for such a large value of δ . We have optimized E_{tot} similarly for various values of δ , and depict in Fig.3(a) the difference of E_{tot} between the d and ext. d waves, $\Delta E = E_{\text{tot}}^d - E_{\text{tot}}^{\text{ext}.d}$.²⁶ In electron-doped cases, the ext. d wave is always more stable than the d wave. The large value of ΔE near half filling probably stems from the fact that the Gaussian peaks in $\Delta_{\mathbf{k}}^{\text{ext}.d}$ are close to the hot spots, as well as that the energy scale in the condensation energy $E^{\text{cond}} (= E_{\text{tot}}^{\text{normal}} - E_{\text{tot}}^{\text{SC}})$ becomes large for $\delta \rightarrow 0$. ΔE vanishes at $\delta = 0.222$, where the hot spots still survive, but E^{cond} vanishes for both waves. Conversely, in the hole-doped cases [open symbols in Fig.3(a)], the simple d wave is more stable than the ext. d wave except in the vicinity of half filling. In the optimal- and overdoped regime for $\delta < 0$, the hot spots sit near $(\pi, 0)$ and equivalent points, whereas near half filling the hot spots are still away from $(\pi, 0)$ point and rather closer to the Gaussian positions we set [Fig.1(b)]. Thus, the results in E_{tot} definitely indicate that the SC state becomes stable when the maximum of the gap $\Delta_{\mathbf{k}}$

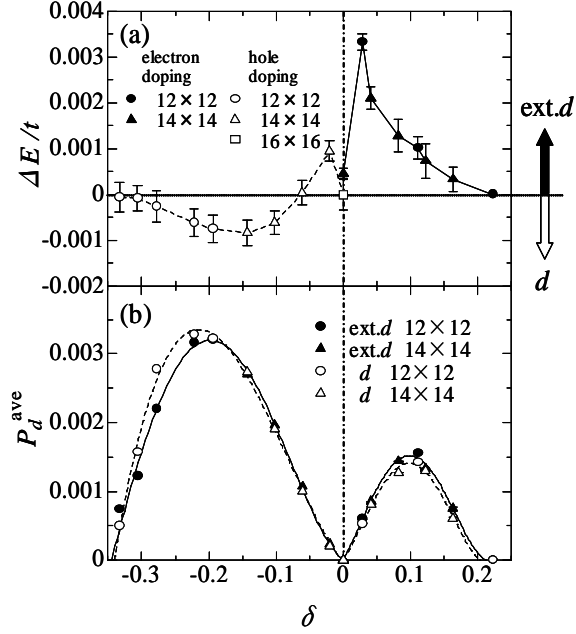


Fig. 3. (a) Difference in the optimized energy between the ext. d - and simple d -wave states, $\Delta E = E_{\text{tot}}^d - E_{\text{tot}}^{\text{ext.}d}$, as a function of doping rate δ . Since the parameters (t' and t'') are different between p and n types, the values at $\delta = 0$ do not coincide. (b) Comparison of the pair correlation function between the ext. d and simple d waves as a function of δ . In both panels, hole-doped systems are indicated by negative values of δ .

is located near the hot spots of the system.

To reinforce the above argument, we consider the d -wave SC correlation function of nearest-neighbor pairs,

$$P_d(\mathbf{r}) = \frac{1}{N_s} \sum_{\mathbf{j}} \sum_{\tau, \tau' = \mathbf{x}, \mathbf{y}} (-1)^{1-\delta(\tau, \tau')} \langle \Delta_{\tau}(\mathbf{j}) \Delta_{\tau'}(\mathbf{j} + \mathbf{r}) \rangle,$$

with $\Delta_{\tau}^{\dagger}(\mathbf{j}) = (c_{\mathbf{j}\uparrow}^{\dagger} c_{\mathbf{j}+\tau\downarrow}^{\dagger} + c_{\mathbf{j}+\tau\uparrow}^{\dagger} c_{\mathbf{j}\downarrow}^{\dagger})$. Since $P_d(\mathbf{r})$ rapidly decays with $|\mathbf{r}|$ and is almost constant for $|\mathbf{r}| \geq 3$, the average for $|\mathbf{r}| \geq 3$, P_d^{ave} , gives an adequate estimate of the long-distance value. In Fig.3(b), P_d^{ave} is plotted versus carrier density. The remarkable asymmetry between the p and n types can be attributed to the difference in DOS at the Fermi surface,²⁷ particularly at the hot spots. Note that the ext. d wave always exceeds the d wave for the n type, whereas the relation is inverse in the over-doped regime for the p type. This tendency of $P_d(\mathbf{r})$ corresponds well with that of ΔE [Fig.3(a)]. Incidentally, in n -type systems, the SC correlation of long-distance pairs is probably enhanced, as will be discussed later.

Next, to identify the origin of the energy gain in E_{tot} , we compare the energy components, namely hopping energy $E_t = \langle \mathcal{H}_t \rangle$ and exchange energy $E_J = \langle \mathcal{H}_J \rangle$, among the d -wave, ext. d -wave and normal states. In Table I, we list the raw values of the d -wave, E_t^d and E_J^d , and the differences between them and those of the other two states, namely, $\Delta E_t^N (= E_t^d - E_t^{\text{normal}})$, $\Delta E_t (= E_t^d - E_t^{\text{ext.}d})$, etc. for four kinds of doping. As compared with the normal state, the d - (also ext. d -) wave SC state is stabilized by the noticeable decrease in E_J ; conversely, E_t is more or less increases. Such magnetic origin of superconductivity is characteristic of t - J -type models,^{18,28} and

Table I. Comparison of the energy components, E_t and E_J , for four carrier densities with $J/t = 0.3$ and t being the unit. The energy components of the simple d wave, E_t^d and E_J^d , are entered in the first two lines. Entered in the middle and lower two lines are the differences of E_t and E_J between the d -wave and the normal state and between the d and ext. d waves, respectively.

δ	-0.143	-0.061	0.082	0.163
E_t^d	-0.3541(1)	-0.1634(1)	-0.2314(1)	-0.4593(1)
E_J^d	-0.2336(1)	-0.2876(0)	-0.2566(1)	-0.1946(0)
ΔE_t^N	0.0090(5)	0.0066(4)	0.0151(2)	0.0043(2)
ΔE_J^N	-0.0288(2)	-0.0471(2)	-0.0313(2)	-0.0052(1)
ΔE_t	-0.0005(2)	-0.0008(2)	-0.0008(2)	-0.0014(2)
ΔE_J	-0.0004(1)	0.0008(1)	0.0021(1)	0.0018(1)

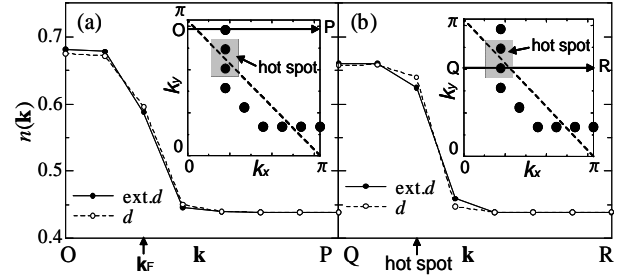


Fig. 4. Comparison of the momentum distribution function between the ext. d and pure d waves along the path indicated by an arrow in each inset, for the electron-doped system with $\delta = 0.122$. In each inset, solid dots and a broken line denote the outmost occupied k -points (the Fermi surface) due to $\varepsilon_{\mathbf{k}}$ and the AF Brillouin zone boundary, respectively. The system is of 14×14 .

closely related to the kinetic-energy-driven SC mechanism in the strong-correlation regime of the Hubbard model.²⁹ In comparison of the d and ext. d waves, $E_J^{\text{ext.}d}$ is lower whenever the ext. d wave has a lower total energy ($\delta \gtrsim -0.06$), whereas the ext. d wave always possesses somewhat higher E_t . Thus, the gap structure of the ext. d wave has further advantages to gain magnetic energy for n -type cases over the simple d wave.

Now, we consider the momentum distribution function, $n(\mathbf{k}) = 1/2 \sum_{\sigma} \langle c_{\mathbf{k}\sigma}^{\dagger} c_{\mathbf{k}\sigma} \rangle$, to actually observe the gap behavior in the momentum space—a milder slope at quasi- k_F . In Figs. 4(a) and (b), we depict $n(\mathbf{k})$ for an electron-doped case³⁰ along two paths, namely OP [in (a)], which goes away from the hot spots, and QR [in (b)], which penetrates the hot-spot area. In (a), $n(\mathbf{k})$'s for the d and ext. d waves exhibit similar behavior, and the d wave seems slightly mild. On the other hand, in (b) the ext. d wave makes an obviously milder curve around the hot spot. Thus, the gap behavior around the hot spot is enhanced in the ext. d -wave state. Incidentally, in the node-of-gap direction, $(0,0)$ - (π, π) , the difference between the d and ext. d waves is very small, and a clear Fermi surface [discontinuity in $n(\mathbf{k})$] can be seen (not shown).

Finally, we consider the spin correlation function. In Fig.5(a), the spin structure factor, $S(\mathbf{q}) = 1/N_s \sum_{\mathbf{i}, \mathbf{j}} e^{i\mathbf{q} \cdot (\mathbf{i} - \mathbf{j})} S(\mathbf{i}, \mathbf{j})$ with $S(\mathbf{i}, \mathbf{j}) = \langle S_i^z S_j^z \rangle$, of the d and ext. d waves is plotted for several densities of electron doping. Both waves have the maximal amplitude at (π, π) for all the electron densities, which is consistent

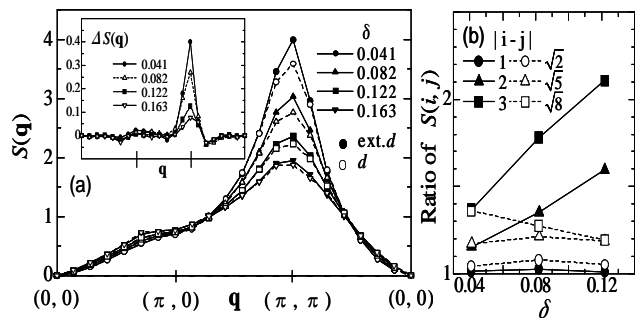


Fig. 5. (a) Comparison of the spin structure factor between the ext. d and pure d waves along the path $(0,0) \rightarrow (\pi,0) \rightarrow (\pi,\pi) \rightarrow (0,0)$ for four densities of electron doping. Plotted in the inset is the difference of $S(\mathbf{q})$ between the d and ext. d waves, $\Delta S(\mathbf{q}) = S^{\text{ext.}d}(\mathbf{q}) - S^d(\mathbf{q})$. (b) Ratio of real-space spin correlation function between the d and ext. d waves, $S^{\text{ext.}d}(\mathbf{i},\mathbf{j})/S^d(\mathbf{i},\mathbf{j})$, is plotted for several values of $|\mathbf{i}-\mathbf{j}|$ as a function of δ . The data shown are the average among the four (or eight) equidistant sites. The system is of 14×14 .

with the neutron experiment.³ As shown in the inset of Fig.5(a), the difference between the d and ext. d waves is almost restricted to the vicinity of (π,π) , where $S(\mathbf{q})$ of the ext. d wave is sizably enhanced. This enhanced AF correlation naturally leads to the energy gain in E_J , mentioned above. Shown in Fig.5(b) is the ratio of the real-space spin correlation function for the ext. d wave to that for the simple d wave. Although the d and ext. d waves exhibit almost the same values for the nearest-neighbor sites ($|\mathbf{i}-\mathbf{j}| = 1$), $S(\mathbf{i},\mathbf{j})$ of the ext. d wave for farther distances considerably increases, especially in the x (or y) direction. This is because the harmonics of the d wave, $\cos nk_x - \cos nk_y$ ($n \geq 2$), give substantial contribution to $\Delta_{\mathbf{k}}^{\text{ext.}d}$.¹¹ Unlike the pure d wave ($n = 1$), they elongate the coherence length (and magnetic correlation length); thereby the correlation strength in the electron-doped systems becomes effectively weaker.³¹ Such tendency has been actually observed by various experiments.³²

Summary: Using a variational Monte Carlo method for a t - J model, we have studied a nonmonotonic (ext.) d -wave superconducting state, in which the amplitude of the gap parameter $\Delta_{\mathbf{k}}$ is intentionally enhanced around the hot spots, so as to agree with recent experiments of Raman scattering and ARPES. This ext. d -wave state has an appreciably lower energy than the simple d -wave state for all the densities of electron doping (also very low hole doping). This stabilization of the ext. d wave is caused by the gain in magnetic exchange energy, accompanied by a marked increase in the spin correlation of the wave vector $\mathbf{Q} = (\pi,\pi)$. In addition, we have shown that the s -type and p waves are unlikely to take place in the high- T_c regime of δ . Our results using a strong-coupling approach basically agree with the recent FLEX study;¹¹ thereby, it is ensured that the AF spin correlation plays a crucial role for the high- T_c superconductivity.

We believe that the essence of the nonmonotonic d -wave gap is grasped in this work, although we have simplified $\Delta_{\mathbf{k}}^{\text{ext.}d}$ by both a naive assumption of a Gaussian form and fixing the parameters controlling the Gaussian. We should address quantitative refinement as well as re-

lated issues. For instance, (1) simultaneous optimization of all the variational parameters, including the renormalization of the quasi-Fermi surface, enables us to follow the continuous evolution of $\Delta_{\mathbf{k}}$ versus δ . (2) The relation to the AF ordered state is very important.

Acknowledgments: One of the authors (H.Y.) appreciates useful discussions with M. Ogata. This work is partly supported by Grant-in-Aids from the Ministry of Education etc., by the Supercomputer Center, ISSP, University of Tokyo, by the 21st Century COE "Frontiers of Computational Science", and by NAREGI Nanoscience Project.

- 1) P. W. Anderson: Science **235** (1987) 1196.
- 2) For instance, D. J. Scalapino: Phys. Rep. **250** (1995) 329.
- 3) K. Yamada *et al.*: Phys. Rev. Lett. **90** (2003) 137004.
- 4) C. C. Tsuei and J. R. Kirtley: Phys. Rev. Lett. **85** (2000) 182.
- 5) T. Sato *et al.*: Science **291** (2001) 1517.
- 6) N. P. Armitage *et al.*: Phys. Rev. Lett. **86** (2001) 1126.
- 7) G. Blumberg *et al.*: Phys. Rev. Lett. **88** (2002) 107002; *ibid.* **90** (2003) 149702.
- 8) H. Matsui *et al.*: preprint (cond-mat/0411547).
- 9) N. P. Armitage *et al.*: Phys. Rev. Lett. **87** (2001) 147003.
- 10) H. Matsui *et al.*: Phys. Rev. Lett. **94** (2005) 047005.
- 11) H. Yoshimura and D. S. Hirashima: J. Phys. Soc. Jpn. **73** (2004) 2057; *ibid.* **74** (2005) 712.
- 12) D. Ceperley, G. V. Chester and K. H. Kalos: Phys. Rev. B **16** (1977) 3081; H. Yokoyama and H. Shiba: J. Phys. Soc. Jpn. **56** (1987) 1490.
- 13) For instance, P. W. Anderson *et al.*: J. Phys. Cond. Mat. **16** (2004) R755.
- 14) A. Biswas *et al.*: Phys. Rev. Lett. **88** (2002) 207004.
- 15) J. A. Skinta, M. -S. Kim and T. R. Lemberger: Phys. Rev. Lett. **88** (2002) 207005.
- 16) V. A. Khodel *et al.*: Phys. Rev. B **69** (2004) 144501.
- 17) T. Tanamoto, H. Kohno and H. Fukuyama: J. Phys. Soc. Jpn. **61** (1992) 1886; H. Kontani, K. Kanki and K. Ueda: Phys. Rev. B **59** (1998) 14723.
- 18) H. Yokoyama and M. Ogata: J. Phys. Soc. Jpn. **65** (1996) 3615.
- 19) M. Randeria, A. Paramekanti and N. Trivedi: Phys. Rev. B **69** (2004) 144509.
- 20) The variational energy weakly depends on a, c and d , but has a relatively narrow minimum as a function of b . Thus, the position of the Gaussian peaks has a special significance.
- 21) Experiments on the surface have yielded both affirmative²² and contradictory^{14,15,23} conclusions to the d -type waves. They may be affected by other factors than electronic origin, for instance, surface impurities.²⁴
- 22) For instance, J. D. Kokales *et al.*: Phys. Rev. Lett. **85** (2000) 3696; B. Chesca *et al.*: Phys. Rev. B **71** (2005) 104504.
- 23) For instance, S. Kashiwaya *et al.*: Phys. Rev. B **57** (1998) 8680, L. Shan *et al.*: preprint (cond-mat/0503321).
- 24) Y. Asano, Y. Tanaka and S. Kashiwaya: Phys. Rev. B **69** (2004) 214509.
- 25) H. Yokoyama and H. Shiba: J. Phys. Soc. Jpn. **57** (1988) 2482; C. Gros: Ann. Phys. (New York) **189** (1989) 53. In the present case, the d -type SC states are stable for $-0.35 < \delta < 0.22$.
- 26) We use a negative value of δ for a hole-doped case so as to discuss the p and n types of doping simultaneously.
- 27) C. T. Shih *et al.*: Phys. Rev. Lett. **92** (2004) 227002.
- 28) D. J. Scalapino and S. R. White: Phys. Rev. B **58** (1998) 8222; E. Demler and S. C. Zhang: Nature **396** (1998) 733.
- 29) H. Yokoyama *et al.*: J. Phys. Soc. Jpn. **73** (2004) 1119.
- 30) In n -type cases, $n(\mathbf{k})$ becomes $1/2 \sum_{\sigma} [1 - \langle h_{\mathbf{Q}-\mathbf{k},\sigma}^{\dagger} h_{\mathbf{k},\sigma} \rangle]$ through the canonical transformation.
- 31) Y. Yanase and K. Yamada: J. Phys. Soc. Jpn. **70** (2001) 1659.
- 32) For instance, Y. Hidaka and M. Suzuki: Nature **338** (1989) 635; G. -q. Zheng *et al.*: Phys. Rev. Lett. **90** (2003) 197005.